



April 23, 2022

# A brief review of the theory of charmonium suppression in heavy ion collisions

JACOPO GHIGLIERI<sup>1</sup>

*Physics Department  
McGill University, Montréal, Canada*

A brief overview of the theory of charmonium suppression in heavy ion collisions is presented. In particular I will concentrate on the effects caused by the hot, deconfined medium and on the effort to treat them using field-theoretical, QCD-based techniques, such as lattice QCD and Effective Field Theories.

PRESENTED AT

The 6<sup>th</sup> International Workshop on Charm Physics  
(CHARM 2013)  
Manchester, UK, 31 August – 4 September, 2013

---

<sup>1</sup>The speaker is supported by the Natural Sciences and Engineering Research Council of Canada and by an Institute of Particle Physics Theory Fellowship.

# 1 Introduction

The phase diagram of QCD in the region of vanishing chemical potential is actively explored in heavy ion collision experiments at RHIC and LHC. Lattice calculations (see [1] for a recent review) predict a crossover transition to a larger number of degrees of freedom, typical of a deconfined medium, the Quark-Gluon Plasma (QGP) for temperatures  $T$  ranging from 150 to 200 MeV. On the experimental side, the characterization of the properties of the medium relies either on its bulk properties, which find an effective description in hydrodynamics, or on *hard probes*, i.e. energetic particles not in equilibrium with the medium.

Heavy quarkonium has been one of the most actively investigated hard probes for the past 27 years. In 1986 Matsui and Satz [2] hypothesized that colour screening in a deconfined medium would have dissociated the  $J/\psi$ , resulting in a suppressed yield in the easily accessible dilepton decay channel and yielding a striking QGP signature. Experimentally, suppression (or lack thereof) is investigated through the *nuclear modification factor*  $R_{AA}$ , defined as the (quarkonium) yield in the nucleus-nucleus collision divided by the corresponding one in  $pp$ , scaled by the number of binary collisions. Heavy ion collision experiments at SPS, RHIC and LHC (see [3, 4] for a review) have indeed reported  $R_{AA} < 1$ . Furthermore the LHC results have opened up the frontier of the cleaner bottomonium probe with the availability of quality data on the  $\Upsilon$  resonances (see [5] for the latest CMS results).

The current theoretical understanding is that all stages of a heavy ion collision contribute to some level to the deviation from simple binary scaling. In the early stages one has to address *cold nuclear matter* effects, i.e. those caused by a confined, nuclear environment. The current understanding is that these effects alone cannot explain the observed  $R_{AA} < 1$ . Later, after a fast thermalization (it is believed to happen in less than 1 fm/c), the system reaches an approximate local thermal equilibrium in the deconfined phase. There one usually speaks of *hot nuclear matter* or *hot medium* effects, such as the aforementioned colour screening. The hot medium is rapidly expanding and cooling down, in a process that is nowadays well described by hydrodynamics (see [6] for a recent review), eventually hadronizing into final state particles, in a time that is estimated to be at most  $\sim 10$  fm/c. At this stage unbound  $c\bar{c}$  pairs might hadronize into a charmonium resonance, in what is known as *statistical recombination* [7]. Any surviving vector state will then decay on a timescale that is several order of magnitude longer than those encountered so far. It is finally worth remarking that, when studying the vector ground states  $J/\Psi$  and  $\Upsilon(1S)$ , one needs to take into account that in a  $pp$  collision roughly one half of the observed yield comes from feed-down from excited states [8]. Medium modifications thereto need then to be consistently taken into account.

In this proceeding we will concentrate on a brief description of some of the issues in the theoretical description of cold and hot nuclear matter effects. Due to the limited

space, we will mostly refer to reviews, such as [9, 3, 10]. The interested reader is invited to follow up on the original references therein. Finally, recent phenomenological transport models which implement, in different manners, a number of the aforementioned effects for charmonia and bottomonia can be found in [11, 12, 13, 14, 15].

## 2 Cold nuclear matter effects

A theoretical description of quarkonium production, even in the cleaner  $pp$ ,  $pe$  and  $e^+e^-$  initial states, is a challenging task (see [3, 16]), which is clearly made no easier by the many-body initial nuclear environment. In the context of explaining deviations from binary scaling, the focus is then to understand how a nucleus differs from  $\sim 200$  nucleons. Schematically, differences appear both before and during/after the collision. In the former case one has to deal with *shadowing*<sup>\*</sup>, i.e. the modification of the Parton Distribution Functions (PDFs) in the nucleus relative to the the single nucleon, and with *energy loss* of the partons before the hard collision event. In the latter case a (quasi)formed  $Q\bar{Q}$  state may be absorbed while traversing the nuclear environment.

The treatment of these effects is mostly phenomenological and data driven. Reviews can be found in [3, 10]. In summary, shadowing is addressed by parametrizing the nuclear PDFs; quark ones can be constrained from  $eA$  deep-inelasting scattering data, whereas the gluon distribution needs to be inferred indirectly. This introduces a sizeable source of uncertainty in these parametrizations. Similarly, nuclear absorption introduces uncertainties in the estimation of the absorption cross sections for the different states and for their precursors, which may also be in a colour octet state. Finally, we also mention that the Color Glass Condensate (CGC) framework (see [17] for a review) can be used to study the initial state effects.

It is on the other hand necessary to remark that such effects, hence the name, also contribute to  $pA$  and  $dA$  collisions, where hot nuclear matter effects are unlikely to occur. Experimental data is available for this asymmetrical collisions at RHIC and LHC and can be used to constrain the theoretical descriptions of these effects. For illustration purposes, Fig. 1 shows the recent ALICE data on  $J/\psi$  production in  $pPb$  collisions [18] and its comparison with theoretical calculations of cold nuclear matter effects and the associated uncertainties.

## 3 Hot nuclear matter effects

As mentioned in the introduction, we are now dealing with the effects caused by a hot, deconfined medium, which were those that motivated the initial hypothesis of Matsui and Satz. Their reasoning was based on colour screening, a well-known property of

---

<sup>\*</sup>Properly speaking, shadowing refers only to the small- $x$  region.

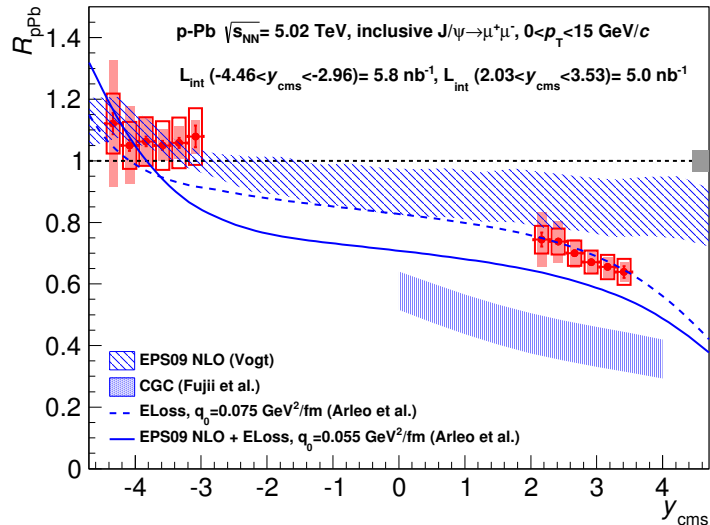


Figure 1: The ALICE data on  $J/\psi$  production in  $pPb$  collision (relative to  $pp$ ) [18] and its comparison with theoretical calculations of cold nuclear matter effects and the associated uncertainties. We refer to [18] for the references on these theory predictions. Figure taken from [18].

plasmas, abelian and non-abelian alike. Since the screening length is approximately inversely proportional to the temperature, in this scenario one expects a sequential suppression, from the less tightly to the more tightly bound states, as the temperature is increased.

We give here a sketch of some modern, QCD-based field-theoretical approaches to the dynamics of a  $Q\bar{Q}$  pair in the QGP. Due to space limitations, recent developments using other approaches, such as AdS/CFT, will not be discussed.

### 3.1 Extracting the spectral function from the lattice

All the relevant information about the in-medium bound state is contained in the spectral function  $\sigma(\omega, \mathbf{p})$  of the relevant local mesonic operator  $J_H(x) \equiv \bar{\psi}(x)\Gamma_H\psi(x)$ , where  $\Gamma_H$  is the appropriate Dirac structure and  $\sigma$  is given by the imaginary part of the Fourier-transformed retarded correlator of  $J_H$ . Being a Minkowskian quantity,  $\sigma$  is not directly accessible on the lattice. One then exploits the following equation

$$G(\tau, \mathbf{p}) \equiv \int d^3x e^{i\mathbf{p}\cdot\mathbf{x}} \langle J_H(\tau, \mathbf{x}) J_H(0, \mathbf{0}) \rangle = \int_0^\infty d\omega \sigma(\omega, \mathbf{p}) \frac{\cosh(\omega(\tau - 1/(2T)))}{\sinh(\tau/(2T))}, \quad (1)$$

which relates the spectral function on the r.h.s. with the Euclidean correlator on the l.h.s. The latter can be measured on the lattice, but the extraction of the former

requires the inversion of the above equation through a Bayesian technique known as the Maximum Entropy Method (MEM), as first performed in [19]. Over the years however it was realized how this approach is prone to systematic effects introduced by the choice of the priors and the low sensitivity of the Euclidean correlator in Eq. (1) to changes in the temperature; recent studies [20] find no charmonium bound states above  $1.5 T_c$ , as shown in Fig. 2. Spatial correlators might also provide a more temperature-sensitive Euclidean probe [21].

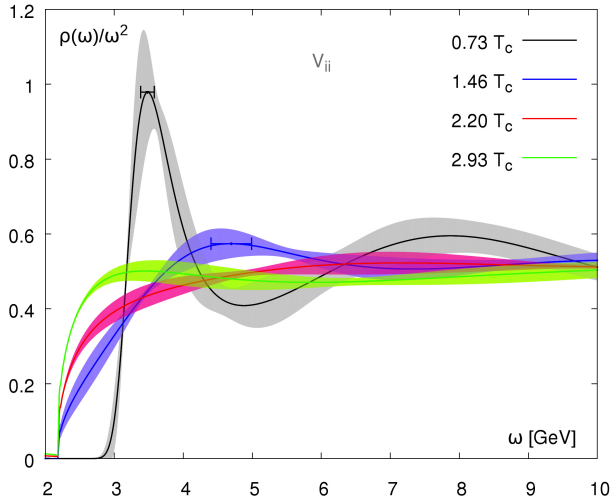


Figure 2: The MEM charmonium spectral function in the vector channel [20]. The shaded bands represent the statistical uncertainties only. Figure taken from [20].

### 3.2 Potential models

Potential models have been and are a very popular approach to the problem. First introduced in [22], they rely on the assumption that all in-medium dynamics can be encoded in a temperature-dependent potential plugged in a Schrödinger equation. A common choice for the potential is the so-called singlet free energy [23], a gauge-dependent correlator of two Polyakov lines which can be easily measured on the lattice in Coulomb gauge. A recent calculation [24] is plotted in Fig. 3 and indeed shows a pattern of increasing screening with the temperature. Other approaches employ the Legendre-transformed internal energy instead, resulting in a more binding potential, resulting in widely varying phenomenological implications for the  $J/\psi$  and other states. We refer to [9, 10] for reviews. Here we just wish to remark that these models are not directly derived from QCD, nor is the specific form of the potential to be used. As we shall discuss in the next section, the Effective Field Theory (EFT) approach addresses these issues.

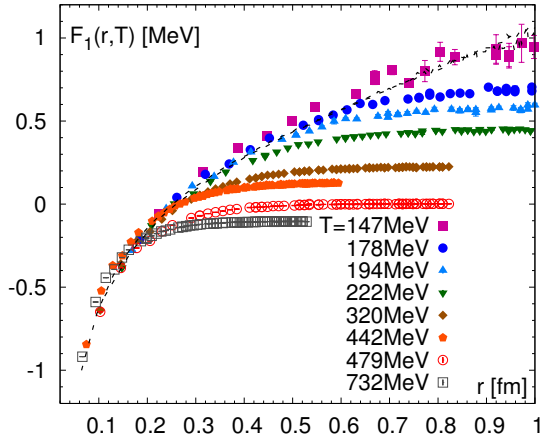


Figure 3: A recent determination [24] of the colour-singlet free energy in Coulomb gauge in  $2 + 1$  flavor QCD. Figure taken from [24].

### 3.3 The EFT approach

This approach is based on the exploitation of scale separations at the Lagrangian level and is inspired from the successful  $T = 0$  framework. There, one makes use of the non-relativistic hierarchy  $m \gg mv \gg mv^2$ , where  $m$  is the heavy quark mass and  $v \ll 1$  the relative velocity. Upon integrating out the scale  $m$  Non-Relativistic QCD (NRQCD) is obtained [25]. The second step is the integration of the scale  $mv$ , which leads to potential Non-Relativistic QCD (pNRQCD) [26]. The relative hierarchical position of  $\Lambda_{\text{QCD}}$  and  $mv$  establishes whether this integration is to be performed perturbatively or non-perturbatively. In the former case the  $Q\bar{Q}$  sector of the Lagrangian reads [26]

$$\begin{aligned} \mathcal{L}_{\text{pNRQCD}} = \int d^3r \text{Tr} \left\{ S^\dagger \left[ i\partial_0 + \frac{\nabla^2}{m} - V_s \right] S + O^\dagger \left[ iD_0 + \frac{\mathbf{D}^2}{m} - V_o \right] O \right. \\ \left. + (O^\dagger \mathbf{r} \cdot g\mathbf{E} S + \text{H.c.}) + \frac{1}{2} O^\dagger \{ \mathbf{r} \cdot g\mathbf{E}, O \} + \dots \right\}, \quad (2) \end{aligned}$$

where  $S$  and  $O$  are the colour-singlet and colour-octet  $Q\bar{Q}$  bilinear field, which appear as the degrees of freedom of the theory. The second line contains their interactions at leading (dipole) order in the expansion for  $mv^2 \ll mv$ . At the zeroth order in that expansion the equation of motion for the singlet field is a Schrödinger equation, with the potential rigorously determined from QCD through the matching procedure. In the strong-coupling case the octet degrees of freedom are integrated out as well, obtaining a Schrödinger picture to all orders.

The extension of this framework to finite temperatures, started in [27, 28] (see

[10, 29] for reviews), requires the introduction of the thermal scales (the temperature  $T$  and the screening masses) in the problem. In phenomenologically relevant situations the heavy quark mass is larger than the temperature,  $m \gg T$ , hence the first step is unchanged and yields standard NRQCD. At this point one can either use this theory directly or proceed to obtain other EFTs. In the former case NRQCD is simulated on the lattice, which has the advantages of making bottomonium physics accessible nonperturbatively and furthermore simplifies the convolution of the spectral function on the r.h.s. of Eq. (1) to a simpler Laplace transform, which is easier to invert with MEM techniques. The results show a survival of the  $S$  bottomonium ground states up to  $\sim 2T_c$  and a rapid disappearance of the  $P$  states after the transition [30].

On the other hand, one can proceed to integrate out other scales. If one assumes weak coupling, then the thermal scales also develop a hierarchy and one has to consider all the relevant scenarios, from  $T \gg mv$  to  $T \lesssim mv^2$  and proceed to systematically integrate out all scales, leaving only  $mv^2$  and smaller scales as dynamical. In all cases, once the scale  $mv$  is integrated out, the resulting EFT resembles pNRQCD and its Lagrangian (2), yielding, similarly to the previous  $T = 0$  discussion, a modern and rigorous definition of the potential. A key feature of the potentials obtained in the different scenarios is that they are *complex* [31, 32, 27], i.e. they contain a sizeable imaginary part that encodes the decoherence effects that interactions with the medium cause; this leads to a thermal width for the state. For instance, for distances of the order of the screening length  $1/m_D$ ,  $m_D^2 = g^2 T^2(1 + n_f/6)$  being the Debye mass, the potential reads [31]

$$V_s(r \sim 1/m_D) = -\frac{4}{3} \frac{\alpha_s}{r} e^{-m_D r} - \frac{4}{3} \alpha_s m_D + i \frac{8}{3} \alpha_s T \int_0^\infty dt \left( \frac{\sin(m_D r t)}{m_D r t} - 1 \right) \frac{t}{(t^2 + 1)^2}. \quad (3)$$

The real part is a screened Debye potential (plus a constant, negative self-energy contribution) and is actually smaller, in the power-counting of the theory, than the imaginary part, highlighting its importance.

Within the weakly-coupled EFT framework one can then proceed to compute medium modifications to the spectra and width (see [29] for a review), which have been found by [30] to be in qualitative agreement with the aforementioned lattice NRQCD results.

In the case where no hierarchical separation is present or assumed between  $T$ ,  $mv$  and  $\Lambda_{\text{QCD}}$  one can integrate out all these scales at once, obtaining, as mentioned before, just a Schrödinger-like singlet sector. This requires a non-perturbative determination of the potential. Recent efforts have shown very promising advancements towards the extraction of the static (infinite mass) complex potential from lattice QCD. In Refs. [33, 34] it has been shown how improvements in the MEM can be used to obtain a potential whose imaginary part, at short distances, is of the same size of the perturbative result [31], as shown in Fig. 4 (a similar approach, although not

relying on MEM, has been very recently reported in [35]). The results also show a dependence on the operator being measured on the lattice: more effort is needed to establish the appropriate ones, also for non-static corrections.

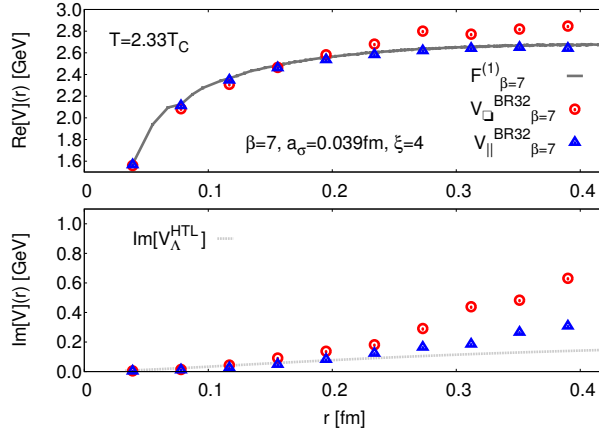


Figure 4: The real and imaginary parts of the potential obtained in [34]. The data points come from different correlators of Wilson lines.  $\text{Im}[V_{\Lambda}^{\text{HTL}}]$  is the perturbative result of [31], as given by Eq. (3). Figure taken from [34].

Phenomenologically, the complex potential yields a broadening of the spectral functions at lower  $T$  than the purely real potential models [36, 37] (see [38] for analogous conclusions in the T-matrix approach). The relation of the imaginary part with earlier approaches in the literature has been investigated in [38, 39]. A model implementing an anisotropic complex potential, coupled to the hydrodynamical evolution of the plasma, has been shown to describe well the LHC  $\Upsilon$  data [11], highlighting the importance of a dynamical description of the medium, while in [40] the possible relevance of vacuum-medium interference effects has been pointed out. The impact of the relative velocity of quarkonium in the plasma has been considered in [41, 42]. We refer to [10] for a wider review of the phenomenological applications.

## 4 Conclusions

We have given a brief overview of some theoretical aspects in the description of quarkonia in heavy ion collisions. The initial stages of the collision are affected by CNM effects, such as shadowing, initial energy loss and nuclear absorption. The approach to these issues is mostly phenomenological; proton(deuteron)-nucleus collisions represent a very useful tool to this end, as these effects are present in those environments too.



For what concerns the hot medium effects, we have summarized some QCD-based approaches. The direct extraction of the  $Q\bar{Q}$  spectral function from the lattice is hampered by the need of an analytical continuation. Nevertheless, qualitative results on dissociation temperatures can be extracted [20, 21]. We have then shown how the long-employed potential models can be brought in contact with QCD using Effective Field Theories [25, 26], which allow for a rigorous QCD derivation of the potential, which turns out to be complex [31, 32, 27], its imaginary part encoding the thermal width caused by interactions with the plasma. The potential can be determined in perturbation theory at weak coupling and recent developments are showing the viability of nonperturbative determinations [33, 34]. Furthermore, NRQCD itself can be put on the lattice [30], which is particularly advantageous for bottomonium.

## References

- [1] P. Petreczky, J. Phys. G **39** (2012) 093002 [arXiv:1203.5320 [hep-lat]].
- [2] T. Matsui and H. Satz, Phys. Lett. B **178** (1986) 416.
- [3] N. Brambilla *et al.*, Eur. Phys. J. C **71** (2011) 1534 [arXiv:1010.5827 [hep-ph]].
- [4] C. Blume, these proceedings.
- [5] S. Chatrchyan *et al.* [CMS Collaboration], Phys. Rev. Lett. **109** (2012) 222301 [arXiv:1208.2826 [nucl-ex]].
- [6] P. Huovinen, arXiv:1311.1849 [nucl-th].
- [7] P. Braun-Munzinger and J. Stachel, Phys. Lett. B **490** (2000) 196 [nucl-th/0007059]. R. L. Thews, M. Schroedter and J. Rafelski, Phys. Rev. C **63** (2001) 054905 [hep-ph/0007323]. L. Grandchamp and R. Rapp, Phys. Lett. B **523** (2001) 60 [hep-ph/0103124], Nucl. Phys. A **709** (2002) 415 [hep-ph/0205305].
- [8] P. Faccioli, C. Lourenco, J. Seixas and H. K. Woehri, JHEP **0810** (2008) 004 [arXiv:0809.2153 [hep-ph]]. D. Acosta *et al.* [CDF Collaboration], Phys. Rev. D **71** (2005) 032001 [hep-ex/0412071]. T. Affolder *et al.* [CDF Collaboration], Phys. Rev. Lett. **84** (2000) 2094 [hep-ex/9910025].
- [9] R. Rapp, D. Blaschke and P. Crochet, Prog. Part. Nucl. Phys. **65** (2010) 209 [arXiv:0807.2470 [hep-ph]]. L. Kluberg and H. Satz, arXiv:0901.3831 [hep-ph]. A. Bazavov, P. Petreczky and A. Velytsky, arXiv:0904.1748 [hep-ph].
- [10] A. Mocsy, P. Petreczky and M. Strickland, Int. J. Mod. Phys. A **28** (2013) 1340012 [arXiv:1302.2180 [hep-ph]].

- [11] M. Strickland, Phys. Rev. Lett. **107** (2011) 132301 [arXiv:1106.2571 [hep-ph]].  
M. Strickland and D. Bazow, Nucl. Phys. A **879** (2012) 25 [arXiv:1112.2761 [nucl-th]].  
M. Strickland, AIP Conf. Proc. **1520** (2013) 179 [arXiv:1207.5327 [hep-ph]].
- [12] X. Zhao and R. Rapp, Phys. Rev. C **82** (2010) 064905 [arXiv:1008.5328 [hep-ph]].
- [13] A. Emerick, X. Zhao and R. Rapp, Eur. Phys. J. A **48** (2012) 72 [arXiv:1111.6537 [hep-ph]].
- [14] T. Song, K. C. Han and C. M. Ko, Phys. Rev. C **85** (2012) 014902 [arXiv:1112.0613 [nucl-th]].
- [15] F. Brezinski and G. Wolschin, Phys. Lett. B **707** (2012) 534 [arXiv:1109.0211 [hep-ph]],  
Phys. Rev. C **87** (2013) 024911 [arXiv:1210.8366 [hep-ph]].
- [16] M. Butenschön, these proceedings.
- [17] L. D. McLerran, Lect. Notes Phys. **583** (2002) 291 [hep-ph/0104285].
- [18] B. B. Abelev *et al.* [ALICE Collaboration], arXiv:1308.6726 [nucl-ex].
- [19] M. Asakawa and T. Hatsuda, Phys. Rev. Lett. **92** (2004) 012001 [hep-lat/0308034].
- [20] H. T. Ding, A. Francis, O. Kaczmarek, F. Karsch, H. Satz and W. Soeldner,  
Phys. Rev. D **86** (2012) 014509 [arXiv:1204.4945 [hep-lat]].
- [21] F. Karsch, E. Laermann, S. Mukherjee and P. Petreczky, Phys. Rev. D **85** (2012)  
114501 [arXiv:1203.3770 [hep-lat]].
- [22] F. Karsch, M. T. Mehr and H. Satz, Z. Phys. C **37** (1988) 617.
- [23] S. Nadkarni, Phys. Rev. D **34** (1986) 3904.
- [24] A. Bazavov and P. Petreczky, arXiv:1211.5638 [hep-lat].
- [25] W. E. Caswell and G. P. Lepage, Phys. Lett. B **167** (1986) 437. G. T. Bodwin,  
E. Braaten and G. P. Lepage, Phys. Rev. D **51** (1995) 1125 [Erratum-ibid. D **55**  
(1997) 5853].
- [26] A. Pineda and J. Soto, Nucl. Phys. Proc. Suppl. **64** (1998) 428 [arXiv:hep-ph/9707481].  
N. Brambilla, A. Pineda, J. Soto and A. Vairo, Nucl. Phys. B **566** (2000) 275 [arXiv:hep-ph/9907240],  
Rev. Mod. Phys. **77** (2005) 1423 [hep-ph/0410047].

- [27] N. Brambilla, J. Ghiglieri, A. Vairo and P. Petreczky, Phys. Rev. D **78** (2008) 014017 [arXiv:0804.0993 [hep-ph]].
- [28] M. A. Escobedo and J. Soto, Phys. Rev. A **78** (2008) 032520 [arXiv:0804.0691 [hep-ph]].
- [29] J. Ghiglieri, PoS ConfinementX (2012) 004 [arXiv:1303.6438 [hep-ph]].
- [30] G. Aarts *et al.*, Phys. Rev. Lett. **106** (2011) 061602 [arXiv:1010.3725 [hep-lat]], JHEP **1111** (2011) 103 [arXiv:1109.4496 [hep-lat]], arXiv:1310.5467 [hep-lat]. S. Kim, P. Petreczky and A. Rothkopf, arXiv:1310.6461 [hep-lat].
- [31] M. Laine, O. Philipsen, P. Romatschke and M. Tassler, JHEP **0703** (2007) 054 [arXiv:hep-ph/0611300].
- [32] A. Beraudo, J. -P. Blaizot and C. Ratti, Nucl. Phys. A **806** (2008) 312 [arXiv:0712.4394 [nucl-th]].
- [33] A. Rothkopf, T. Hatsuda and S. Sasaki, Phys. Rev. Lett. **108** (2012) 162001 [arXiv:1108.1579 [hep-lat]]. Y. Burnier and A. Rothkopf, Phys. Rev. D **86** (2012) 051503 [arXiv:1208.1899 [hep-ph]].
- [34] Y. Burnier and A. Rothkopf, Phys. Rev. Lett. **111** (2013) 182003 [arXiv:1307.6106 [hep-lat]].
- [35] A. Bazavov and P. Petreczky, talk by P.P. at Hard Probes 2013, Stellenbosch, South Africa.
- [36] M. Laine, JHEP **0705**, 028 (2007) [arXiv:0704.1720 [hep-ph]]. Y. Burnier, M. Laine and M. Vepsalainen, JHEP **0801** (2008) 043 [arXiv:0711.1743 [hep-ph]].
- [37] P. Petreczky, C. Miao and A. Mocsy, Nucl. Phys. A **855** (2011) 125 [arXiv:1012.4433 [hep-ph]].
- [38] F. Riek and R. Rapp, New J. Phys. **13** (2011) 045007 [arXiv:1012.0019 [nucl-th]].
- [39] N. Brambilla, M. A. Escobedo, J. Ghiglieri and A. Vairo, JHEP **1112** (2011) 116 [arXiv:1109.5826 [hep-ph]], JHEP **1305** (2013) 130 [arXiv:1303.6097 [hep-ph]].
- [40] J. Casalderrey-Solana, JHEP **1303** (2013) 091 [arXiv:1208.2602 [hep-ph]].
- [41] M. A. Escobedo, J. Soto and M. Mannarelli, Phys. Rev. D **84** (2011) 016008 [arXiv:1105.1249 [hep-ph]]. M. A. Escobedo, F. Giannuzzi, M. Mannarelli and J. Soto, Phys. Rev. D **87** (2013) 114005 [arXiv:1304.4087 [hep-ph]].
- [42] G. Aarts *et al.*, JHEP **1303** (2013) 084 [arXiv:1210.2903 [hep-lat]].